Metascience in Aerospace, 3(1): 1–14.
DOI: 10.3934/mina.2026001
Received date: 03 August 2025
Revised date: 19 January 2026
Accepted date: 27 January 2026
Published date: 11 February 2026

https://www.aimspress.com/journal/mina

Research article

Thrust from electric devices as source for anomalous effects on space probes

Elio B. Porcelli* **and Victo S. Filho**

H4D Scientific Research Laboratory, São Paulo, SP 04674-225, Brazil

* **Correspondence:** Email: elioporcelli@h4dscientific.com.

Abstract: Telemetry data have confirmed that the space probes Pioneer 10 and Pioneer 11 experienced anomalous accelerations. A possible explanation for this phenomenon involves thermal effects, based on estimates, approximations, simulations, and several assumptions. Motivated by successful results obtained in similar electric devices, such as the traveling-wave tube amplifier (TWTA) in the probes, we propose an alternative explanation within our theoretical framework based on generalized quantum entanglement, assuming its existence between the onboard TWTA and the external environment. We simulated the operation of this device in the laboratory by manipulating an electron beam. As a result, an anomalous acceleration was detected, and its magnitude was shown to be consistent with our predictions derived from simple models using classical macroscopic observables and known physical parameters from spacecraft designs. The characterization of this novel property paves the way for its application to space propulsion without the ejection of electrons, ions, or propellant gases.

Keywords: electric thrust; space probes; quantum entanglement; pioneers; TWTA

1. Introduction

The main objective of this work is to show that it is possible to generate thrust without propellant exhaust or ion acceleration, and that such anomalous forces can explain route deviation observed in some space probes. Certain closed-system electric devices, such as electromagnetic drives (EM drives) [1,2], are generally considered to contradict the law of conservation of momentum and to violate Newton's third law [3]. However, our recent studies support the view that truly closed systems do not exist when one considers the possibility of a preexisting quantum state of generalized entanglement between all existing particles [4–6]. In fact, our previous works [7–14] have shown that the hypothesis of quantum correlations between the internal particles of devices, such as capacitors, rotors,

magnetrons, and others, and external particles in the nearby environment can consistently explain the existence of anomalous forces or small thrusts verified in experiments involving such devices under strong applied fields. This theoretical framework was analyzed in greater depth in [5–7].

Some quantum effects at the macroscopic scale seem to be extremely weak, but they can be locally amplified under special conditions in which large numbers of electric dipoles in dielectrics, magnetic dipoles in solenoids, or moving electric charges in conductors or superconductors transition collectively to the same quantum state due to strong local fields, such as electric or magnetic fields. This explains why previously unexpected thrusts have been measured in different electric devices, such as solenoids [5], capacitors [7,8], electromagnetic cavities [9], magnetic rotors [10], dielectric rotors [11], semiconductor laser diodes [12,13], and superconductor devices [14,15]. It is relevant to note that in some devices, such as capacitors, the weak force is generated by electric dipoles, whereas in others, such as laser diodes, the source of the anomalous weak force is the electron beam. The latter case is similar to that of space probes, in which an electric current is involved in the physical system.

Based on these studies, we conclude that the existence of weak thrust generated by the operation of such electric devices is well supported. This has motivated us to proceed with more advanced experimental setups in order to obtain higher thrust levels for applications in the aerospace industry. However, in outer space, where friction is negligible, the thrust levels measured in our experiments would already be sufficient to accelerate a spacecraft so that it could reach, for example, Mars.

This small effect also encouraged us to investigate the deviations on the routes of space probes observed after many years of travel in outer space [16–18]. The so-called Pioneer anomaly [16] was first reported in 1998 by Anderson et al., who found from radiometric data that both probes experienced an apparent constant anomalous acceleration of approximately 8.5×10^{-8} cm/s^2, directed toward the Sun. This anomaly refers to the discrepancy between theoretical route predictions and the data sent by both probes. In [17], an alternative explanation was proposed in terms of an acceleration of the clocks $a_t = a_P / c$, in which the index P refers to any probe. The authors obtained $a_t \backsimeq (2.9 \pm 0.4) \times 10^{-18}$ s^{-1}, whereas Anderson et al. reported $_t \backsimeq 1.8 \times 10^{-18}$ s^{-1}. This discrepancy, ranging from approximately 39% to 83% when taking the latter as the most reliable result, clearly leaves room for further investigation. In [18], Anderson's group reported a more profound research of the original effect detected in [16], improving the anomalous acceleration to 8.74×10^{-8} cm/s^2 using additional data, but acknowledging that no systematic origin of the residuals could be identified. The anomaly has been interpreted as a failure of the inverse-square law of gravitation in the framework of general relativity, manifesting in the dynamics of the outer Solar System. Explanations for such an anomaly were also proposed, based on waste heat emitted by the radioisotope thermoelectric generators (RTGs) [19], the spacecraft's electrical subsystems [20], or both [21], motivating a thorough investigation of the spacecraft systematics [22]. In [23], a complete finite-element thermal model of the Pioneer 10 spacecraft was proposed, assuming a thermal origin and a constant acceleration allowing route correction. However, this model relies extensively on the project and spacecraft design documentation, was validated using redundant flight telemetry data, and incorporated a parameterized thermal-force model [24] into Doppler analyses, so that only an estimate of coefficients characterizing the thermal recoil force was obtained.

In the present work, we investigate whether the effect can be explained within our theoretical model based on generalized quantum entanglement (GQE). While the effect has so far been attributed to complex thermal effects, we present a simpler, alternative explanation.

The onboard travelling-wave tube amplifier (TWTA) devices of Pioneer 10 and Pioneer 11 operate using electron beams, which constitute the root cause of the anomalous acceleration in our

framework. This encouraged us to carry out experiments using electron beams to confirm the existence of thrust and to characterize it accordingly. These experiments, as well as the corresponding theoretical development, are described in our paper and show agreement within measurements.

Finally, we analyze the technical specifications of the TWTAs and of the Pioneer, leading to the conclusion that the anomalous acceleration can be explained both qualitatively and quantitatively by our theoretical framework.

2. Materials and methods

We have performed numerous experiments involving different electric devices, mainly investigating thrust, as reported in [5,7–15]. In the case of capacitors subjected to high voltage, a weak anomalous force was detected that decreases their weight [7,8]. The same weight-reduction effect was observed in magnetic cores [5] when subjected to intense magnetic fields.

Other investigated devices and physical systems include rotors [10,11], lasers [12,13], and superconductors [14,15] subjected to high voltage. A similar effect was theoretically analyzed for EM drives [9], indicating the possible magnitude of thrust generated by such devices. The theoretical models based on the GQE hypothesis were constructed and showed good agreement with experimental values measured for the magnetron drive [9]. Each device was systematically characterized in order to understand the technical parameters that determine the magnitude and behavior of the produced thrust.

In order to specifically focus on the characterization of longitudinal forces generated by electron beams in travelling-wave tube amplifiers (TWTA), we conducted experiments using two electrodes enclosed in a hollow tube, in order to rule out any effect related to the ion wind. Electrodes were powered either by a high-voltage power supply (direct current) or by a stun gun (pulsed direct current) via insulated wires.

The hollow tube was placed horizontally on a support placed on a smooth surface. An accelerometer was coupled above the tube using another support, with its Y-axis aligned parallel to the electron beam, as shown in Figure 1.

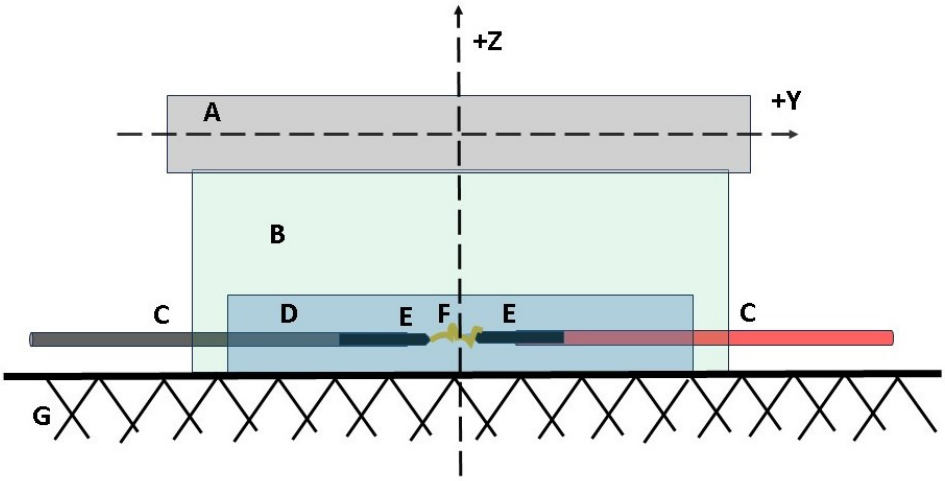

Figure 1. Experimental diagram used in our work. A is the accelerometer supported on the block (B) coupled in the hollow cylinder (D), where the electrodes (E) are placed inside. G is the smooth surface, F is the electron beam (spark), and C is the insulated wires.

The plastic chamber had a diameter of 2 cm and a length of 13 cm. Environmental parameters—temperature, pressure, and humidity—were, on average, 22 °C, 923 hPa, and 68%, respectively. The DC power supply had a 20 W power and a 30 kV maximum output voltage.

The MEMS accelerometer, with a resolution of 0.0001 g, was configured to a collection rate of 100 Hz. During the first seconds of each measurement, data were recorded with the electron beam switched off. In the subsequent period, measurements were taken with the electron beam switched on, at which point sparks across the 1.5 cm gap between the separated electrodes were clearly visible.

The change in acceleration between the on and off periods was obtained by analyzing the average of 100 samples per second from the accelerometer data log (CSV file). Multiple runs were performed.

It was clearly observed that the "anomalous" acceleration occurred when the electron beam was switched on, with its vector pointing in the same direction as the electron flow. Reversing the electron flow direction from +Y to -Y, and vice versa, was achieved by changing the electrode polarization.

By comparing the average of measurements over 8 s during the on period with that over 8 s during the off period, an acceleration magnitude (module) of 0.00578 m/s² was obtained for electrons flowing in the +Y direction. Similarly, a magnitude of 0.00931 m/s² was measured for electrons flowing to the -Y direction when the electrodes were powered by the high-voltage power supply (DC).

Our theoretical framework requires knowledge of the electron-beam current magnitude to forecast the magnitude of the longitudinal force. Accordingly, the current magnitude related to the electron beam was measured using a PA-622 current probe connected to the input channel of a Tektronix TBS1102B oscilloscope, and also on one of the supply wires connected to the electrode powered by the high-voltage power supply (DC). Isolated current peaks of up to 550 A were measured, as shown in Figure 2.

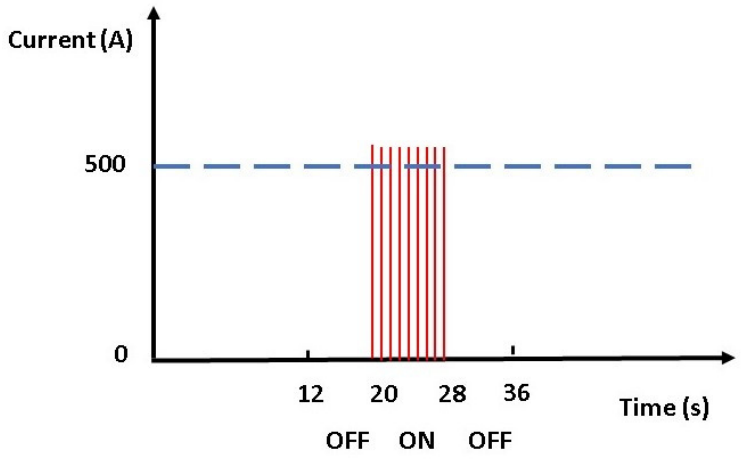

Figure 2. Periods of 8 s of current peaks; some surpassing 500 A when the power supply was switched on. Accelerometer measurements were taken both with the power on and off.

According to the amplitudes of the 10 current peaks (I_{pk}), each with a width of 0.83 ms and an analyzed period of 1.39 s, it is possible to calculate the rms value of the current (I_{rms}) by averaging all peaks and applying, for each one, the equation

$$I_{rms} = \sqrt{I_{pk}^2 \, (t_1 + t_2 \, + \, 3 \, t_o \,) \, / \, 3 \, t} \quad ,$$

where t_o is the peak width, t is the time interval between the peaks, t_1 is the time of the up ramp, and t_2 is the time of the down ramp [25]. Considering that $t_1 << t_o$ and $t_2 << t_o$, it is assumed that $t_1 \sim t_2 \sim 0$. This yields an rms current value of 46.94 A when the electron beam is switched on.

According to GQE theory, all particles in the Universe are in the quantum state of mutual entanglement, and their dynamics are governed by the joint function $| \psi >$, as described by the Schrödinger equation

$$i\hbar \frac{d}{dt} \big| \psi \, > = \, \hat{H} \big| \psi \, > . \tag{1}$$

The time evolution of $| \psi >$ depends on the Hamiltonian $\hat{H}$, which represents the sum of the local binding energies governing each particle. The dynamics of any given particle depend on both its local interactions and nonlocal interactions, i.e., its interactions with all other particles in the Universe. Therefore, for an electron, the Hamiltonian may be written as $\hat{H} = \hat{H}_{\text{electron}} + \hat{H}_{\text{others}}$, where $\hat{H}_{\text{electron}}$ governs its local dynamics, and $\hat{H}_{\text{others}}$ represents the collective contribution of all other particles. The Hamiltonian $\hat{H}_{\text{electron}}$ describing the dynamics of an electron in an electromagnetic field can be represented by the following equation:

$$\hat{H}_{electron} = \frac{1}{2m} \left[-i\hbar\nabla + \mathrm{e}\vec{A}(\vec{r}) \right]^2 + e\emptyset(\vec{r}) + V(\vec{r}). \tag{2}$$

From left to right, after $1/(2m)$ (where m is the mass of the electron), the terms are related to kinetic energy, magnetic vector potential, electric potential, and a possible non-electric potential, respectively. The first two terms represent the kinetic contribution of the Hamiltonian and are the most relevant in this study, as they represent the changes in electron kinetic energy and momentum according to its interaction with the electromagnetic field. As described by Aharonov and Bohm [26], a moving electron in a solenoid can change the phase of the wave function of external electrons and can even exert a force on them, as demonstrated in a recent experiment [27], without mediation by a field. This is an intrinsic nonlocal phenomenon, predicted by quantum mechanics, in which the longitudinal mode of the magnetic vector potential $\vec{A}$ determines the dynamics of other particles. The magnetic vector potential is parallel to the direction of movement of an electron (indeed, its source) that moves in a straight conductor; the same occurs in a current where many electrons move in an orderly manner.

At the macroscopic scale, classical variables [28] and a quantum mechanical approach [29] can be combined to calculate the magnitude of longitudinal force F by considering the anti-symmetric wave functions of electrons and their statistical collective distribution (Fermi). The kinetic energy is defined by

$$E_k = \frac{1}{2} \left(\frac{ml}{ne^2 A} \right) I^2,$$

where $I = nevA$ is the current, and the total electron mass is $M = mnAl$, considering the kinetic energy of the total mass $E_k = \frac{1}{2} M v^2$, where I is the current, m is the electron mass, l is the length where the electrons move, e is the electron charge, v is the Fermi velocity drift of electrons, M is the total electron mass, A is the cross-section area, and n is the Fermi number density. The kinetic energy is related to the work along length l, so that the longitudinal force F can be calculated by the derivation $F = \frac{dE_k}{dl} = \left(\frac{m}{ne^2 A} \right) I^2 \cong \mu_0 I^2$.

From this result and our previous studies [9,12–15], the thrust produced by an electric device in which there is a rms current I is governed by

$$F = \mu_0 G I^2. \tag{3}$$

Here, F is the longitudinal thrust (in Newton), which is proportional to the square value of the current (I^2), and the parameter G corresponds to the gain rate of the current (or gain factor) and to the value of vacuum permeability (μ_o) for the electric devices, such as the electromagnetic cavity without dielectric, semiconductor laser diodes, and superconductor devices. Equation (3) is related to a longitudinal force F. The variable G was added to that equation to represent other local interactions that can affect dynamics, such as external magnetic fields acting in the case of TWTA. Such longitudinal force has been researched both theoretically [30] and experimentally [31]. It has been shown that both the longitudinal force due to the longitudinal mode of the magnetic vector potential coupled to the electron flow (current) and the manifestation of a thrust due to its nonlocal coupling with the medium outside of the circuit are purely quantum phenomena.

At the level of the spacecraft component, each individual electron in the TWTA can produce a thrust, and their collective effect produces a macroscopic anomalous thrust. Some individual elements produce asymmetric heat, generating a thermal thrust via a temperature gradient, while the high-gain parabolic antenna reflects solar radiation, contributing with anisotropic radiation pressure. From the component level to the complete system (whole probe) level, the component forces propagate via vector summation in relation to the center of mass, so that the dynamic model for the equation of spacecraft motion can be written as follows:

$$m\ddot{\vec{r}} = \vec{F}_{grav} + \vec{F}_{rad} + \vec{F}_{prop} + \vec{F}_{drag} + \vec{F}_{therm} + \vec{F}_{GQE}, \tag{4}$$

where the terms represent the gravitational force, the propulsion force, the drag forces (significant in the atmosphere of planets, but negligible for the ultra-vacuum condition in deep space), the thermal force, and the force generated by the quantum mechanism described in this paper, with the magnitude given in (3).

In [23], the authors reported that the estimate of the recoil force based on a numerical thermal analysis (Doppler analysis) is approximately 80%; the remaining 20% represents a statistically significant acceleration anomaly not accounted for by conventional forces. Several possible error sources were analyzed that contribute to such uncertainties using radio-metric Doppler and thermal models. For instance, in the case of the Doppler analysis, a significant noise floor exists due to systematic errors, including interplanetary charged particle environments. The higher source of uncertainty in thermal analysis is the unknown change in the properties of the particles generating heat from radioisotopes, which results in differences in fore-aft emissivity and an additional contribution to the recoil force in the spin axis direction. From this level of uncertainty, with 20% not being explained, there is room for the implementation of a new model, represented by the last force in (4), representing the contribution of the quantum level described here due to the quantum entanglement phenomenon.

For the magnitude of the currents mentioned here, the thrust can be calculated via equation (3) with $G = 1$, because there is no other element that affects electron beams (e.g., a resonant cavity where there is a current flow in the case of a semiconductor laser diode). Equation (3) yields 0.002769 N. Considering a mass m of the setup (wires, hollow cylinder, supports, and accelerometer) of 0.5 kg, the acceleration a can also be calculated according to $a = F$ / m, resulting in the theoretical value of

0.005538 m/s². The proximity of this theoretical value to the experimental ones is remarkable, even though some factors that are not fully controlled could affect the measurements.

In this experiment, the reality of the longitudinal force resulting from the electron beam in a closed system (not explainable by current theories, considering that there was no ejection of electrons or plasma ions) was proven. The effect can be interpreted considering that the electrons interact with the external environment via generalized quantum entanglements, maintaining the validity of the principle of conservation of momentum and implying that there are no absolutely isolated systems. Using equation (3), it is possible to theoretically calculate the magnitude of the force, given its good agreement with the measurements.

In space travel, as there is no friction, such weak forces obtained in our experiments could be useful. They could be the source of propulsion of spacecraft after fossil fuel: in outer space, even very weak magnitudes of acceleration (at the order of mgf) could be enough to accelerate them at first, starting at small velocities but progressing to very high velocities. On Earth, due to atmospheric friction, such effects need only to be enhanced to obtain a useful application, as the effect is weak enough to be easily eliminated by higher forces as the friction force, air force, or collisions with small obstacles or barriers.

It should also be noted that experiments showing the existence of quantum entanglement are well established [32]. In relation to the generalized case (GQE), our experiments provide good evidence of its existence. In a more recent work, we showed stronger verification of the existence of GQE using a laser beam and a distant, shielded capacitor, indicating pre-existing quantum entanglement between discrete observables of electric dipoles and photons [33].

3. Results and discussion

The good agreement between the models described in the previous section and the anomalous phenomena observed in electric devices employing electron beams motivated us to analyze the possibility that a similar anomaly in space probes could be caused by quantum mechanisms in the materials constituting the vehicle.

The small effect verified in the space probes Pioneer 10 and Pioneer 11 [17,18], which are travelling near the limits of the Solar System, corresponds to an anomalous acceleration of approximately $8.74 \pm 1.33 \times 10^{-10}$ m/s^2. The weak force is directed toward the Sun and may be caused by the rotation of the probes about their axes or due to the electric instrumentation aboard [17,18]. A widely accepted explanation, proposed in [23], attributes the anomaly to thermal forces. However, the topic is still controversial and leaves room for alternative hypotheses.

According to our previous work, weak forces in electric devices may originate from quantum mechanisms associated with generalized entanglement among all particles of the internal and external systems. This could also be the case for the Pioneer anomaly. We therefore investigated the configuration of the probes and the instrumentation used inside the devices. Our main objective was to verify whether it is possible for such spacecrafts and satellites to have on-board closed-system electric devices that can generate thrust.

The vast majority of spacecrafts and satellites use a type of onboard radio-frequency amplifier called TWTA (traveling-wave tube amplifier) [34], which consists of a tube in which an accelerated, collimated electron beam is produced by the electric potential difference between a cathode heated by a filament (heater) at one end of the tube and an anode. After passing through the anode, the straight beam hits a collector placed at the opposite end of the tube. Figure 3 shows a simplified diagram of the TWTA.

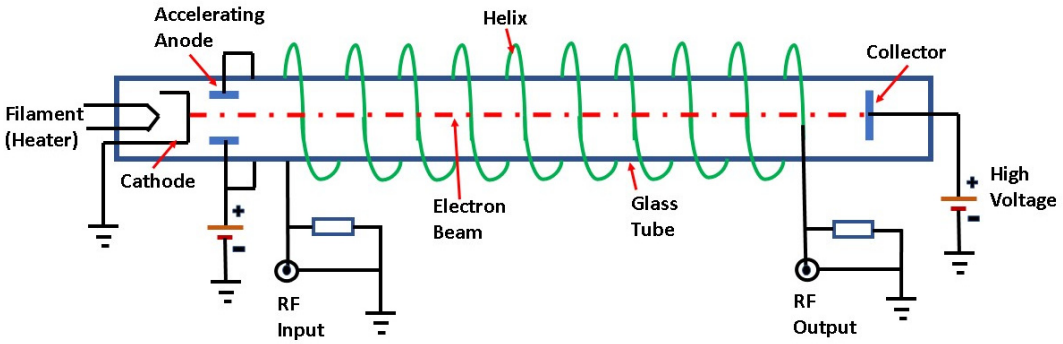

Figure 3. Simplified diagram showing the components of the TWTA, where an electron beam flows from the cathode to the collector accelerated by the intense electric field and whose electrons are bunched due to magnetic interaction with the spiral outer conductor (Helix), where the radio-frequency signal is amplified.

A conductor wraps around the outside of the tube in a helical form. A radio-frequency signal is injected at one end, and the signal is extracted at the other end. An intense magnetic interaction occurs between the radio-frequency signal of the loop (Helix) and the rectilinear beam of electrons. The beam electrons are therefore highly coordinated and bunched [35].

As the electrons of the beam are highly collimated and bunched, as occurs in a linear accelerator of particles, they do not behave like electrons flowing in an ordinary electric current inside a conductor. According to the GQE hypothesis, their interaction with the outside environment under such special conditions is enhanced, considering that the particles are already quantum-entangled and that the system is not perfectly isolated from outer space. Equation (3) should be used to calculate nonlocal forces generated by charges in highly organized motion. This applies to devices such as semiconductor diode lasers, superconductors, electromagnetic cavities associated with magnetrons, accelerators of particles, and, in the present case, the TWTA system of space probes.

Although the electric power of the TWTA used in spacecrafts and satellites is much smaller than that of ground radars and high-gain antennas, it is possible that even a weak force could be measured through the Doppler shift in telemetry signals exchanged with the ground control. Such a detection should be possible mainly in low-mass spacecraft, which have highly stabilized trajectories and attitudes, without frequent or constant corrections.

Most spacecraft do not meet these conditions [35]. However, the anomalous acceleration was detected over decades in Pioneer 10 and 11 without undergoing trajectory corrections (after the Jupiter flyby), and their attitudes were highly stabilized by rotations about their symmetry axes as they traveled toward the outer Solar System.

Figure 4 shows an artistic rendering of these spacecrafts by NASA [36], in which the dish-shaped antenna is always oriented toward Earth, while its magnetometer is supported by a big stem, and its nuclear batteries are supported by smaller stems.

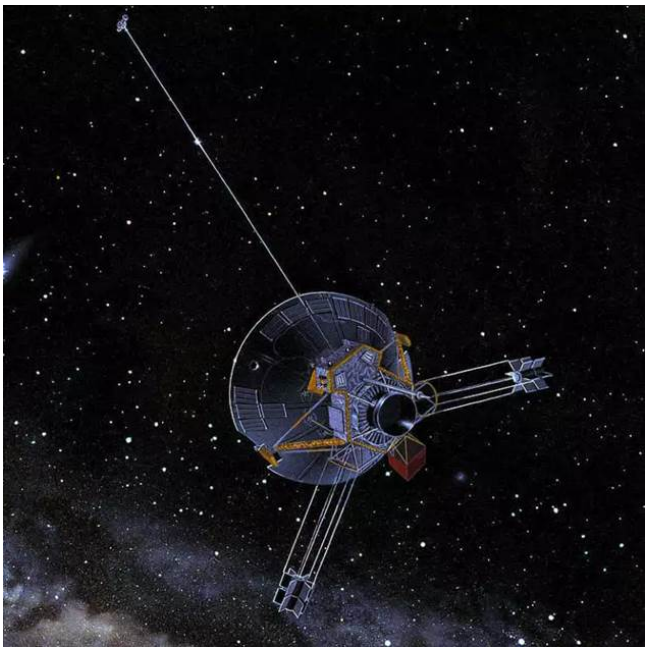

Figure 4. Artistic rendition of the Pioneer 10/Pioneer 11 spacecraft in the outer Solar System. (Credits: Public Domain NASA/Don Davis).

In the study published in 2012 [23], such an anomalous acceleration was attributed to the probes Pioneer 10 and 11 themselves, because their magnitude decreased with the drop in electric power over time, so that they stopped communicating with ground control. Such an effect indicates that the cause of the anomalous acceleration is the nonlocal force F caused by the TWTA onboard the spacecraft, despite the aforementioned study [23] hypothesizing, through estimates and approximations, that the acceleration was caused by the asymmetry in the propagation of radiation thermal emitted mainly by nuclear batteries with its reflection in the spacecraft body (mainly in the dish of the antenna).

The magnitude of the anomalous acceleration in both Pioneer 10 and Pioneer 11 (twin spacecrafts with the same specifications) can be calculated without estimates or approximations by using a few parameters in equation (3) for the nonlocal force generated by the TWTA model WJ - 448 [37], a rated output power of 8 W (operating at S-band frequency), an average electron-beam current I = 79 mA (saturation), and a gain factor G = 30 dB, equivalent to a current gain of 31.62, considering the usual expression 20 log G. Thus, the magnitude of the nonlocal force F calculated through equation (3) is $F = 2.4798 \times 10^{-7}$ N; as the spacecraft mass is m = 260 kg [38], one obtains, via the Newtonian equation, $a = F / m = 9.5379 \times 10^{-10}$ m/s^2.

Such a theoretical magnitude of acceleration is very close to the experimental value of the anomalous acceleration detected in the telemetry of Pioneer 10 and Pioneer 11 [23], which lies in the range 7.41×10^{-10} m/s^2 to 1.007×10^{-9} m/s^2, especially considering that our theoretical calculation assumes a brand new TWTA and that its power dropped over the years.

It is worth understanding how the force of magnitude F acts internally in the spacecraft. The barycenter (center of mass) for Pioneer 10 (and also Pioneer 11) is slightly shifted by its instruments, antennas, and fuel. After its last Jupiter flyby and departure toward the outer Solar System, however, the spacecraft was stabilized approximately around its central axis (z-axis) (around 0.5 rad/s). The TWTAs are placed close to this axis and, therefore, their electron beams are aligned. Because of this,

the torque τ generated by axial forces generated by the TWTAs are approximately null considering τ = $r\,F$ sin θ ~ 0, where r is the radial distance of force applied (r ~ 0), F is the force magnitude, and θ (θ = 90°) is the angle between the force direction and the plane of y- and x-axes (plane of parabolic antenna).

In other words, both the angle of the rotation axis and the angular velocity of the spacecraft remain unchanged. The forces generated by the TWTAs (remembering the nonlocal interaction between their electron beams and the outside environment) applied on the barycenter of the spacecraft are locally, mechanically, and sequentially transmitted through the z-axis by contact with the other solid internal components of the spacecraft [37,38]: the circuit board where the TWTA is connected (F_1), the protective housing (box) of the TWTA (F_2), and the main hexagonal frame supporting the protective housing (F_3). This results in acceleration of the entire spacecraft in the z-direction, so that we have the vector summation of the internal forces $F = \sum_{i=0}^{n} Fi$ representing the TWTA force on the system.

It was also found that the anomalous acceleration always pointed in the opposite direction to the displacement of the spacecraft, that is, there was a deceleration whose vector was parallel to the symmetry axis of the same [23]. This experimental observation also corroborates, without assumptions and estimates, the fact that the effect was caused by the TWTA, due to the position of its electron beam whose flow is parallel to the direction of the anomalous force and also because it points in the same direction to the electronic flow, given that the force generated nonlocal F points in the opposite direction to the displacement of the spacecraft whose attitude is stabilized by the spin, so that the antenna always points toward the Earth.

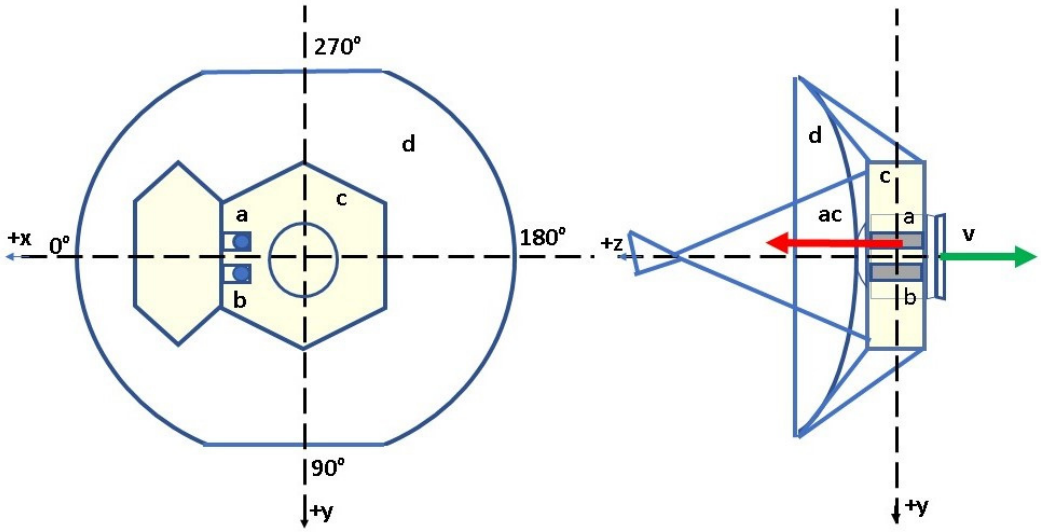

Figure 5. Simplified scheme of Pioneer 10 and Pioneer 11 spacecraft. On the left, the front view of the space probes; on the right, the lateral view. Details of both views are discussed in the main text.

Figure 5, based on [39] and other data used here, shows on its left side the front view of the spacecraft without the magnetometer stem and without the nuclear batteries stems, where the position of the two TWTAs is highlighted (one only works when the other fails, that is, they do not work at the same time). The electron beams are parallel and close to the spacecraft's axis of symmetry. The right

side shows the side view of the spacecraft, where the position of the two TWTAs is also highlighted, indicating that the nonlocal reaction force points are opposite to the spacecraft's displacement vector, parallel to the z-axis (axis of symmetry), which causes the probe to slow down.

Note that the positions of the TWTAs are denoted by points a and b. Point c indicates the position of the spacecraft body, while point d indicates the position of the antenna dish. The vector **ac** is the nonlocal reaction force caused by the activated TWTA, which is parallel to the vector **z** (axis of symmetry), while the vector **v** (spacecraft displacement) is anti-parallel. The stability conditions in the trajectory presented by Pioneer 10 and 11 allow us to corroborate the presence of weak nonlocal forces generated by their TWTAs. In addition, as discussed before, such conditions are difficult to observe in other spacecraft, but perhaps a deeper analysis of the most recent space missions, like NASA's New Horizons spacecraft [40], can provide further evidence.

New Horizons performed several measurements of Pluto and its satellites, including sensational photos. However, prior to reaching this planet, more specifically in the path between Jupiter and Pluto, the spacecraft was in a state of hibernation for years to conserve power and did not undergo path correction [40] to keep its coordinates stabilized and its dish antenna pointing toward planet Earth. Under these conditions, it is possible to detect anomalous accelerations similar to those observed for Pioneer 10 and 11, through analysis of Doppler shifts in the telemetry signals sent by the spacecraft.

As New Horizons was launched much later (January 2006) than Pioneer 10 and 11, it carries more modern and higher-performance TWTAs. Each TWTA, with a rated output power of 12 W, operates in the X frequency band. With a gain G of at least 40 dB, corresponding to a current gain rate of 100 times and an electron beam current magnitude of at least 20 mA (values much more conservative than those of the TWTAs in the Pioneer 10 launch [41]), Equation (3) yields a predicted acceleration of 1.0515×10^{-9} m/s^2, using a spacecraft mass of 478 kg [39]. Such a result motivates a more detailed analysis of the spacecraft telemetry.

These results encourage continued investigation of spacecraft telemetry to examine correlations between TWTA parameters and possible unexpected accelerations. More importantly, they motivate optimization of key parameters, such as gain and magnitude of the electron beam current, so that such closed-system electric devices could be used as true thrusters. The great advantage in TWTAs is that the generated thrust can be increased not only by raising the beam current but also by its gain, a parameter that has been greatly improved in recent decades. The use of high-power TWTA models in spacecraft, currently used in radars and antennas, could be a first step.

4. Conclusions

Our studies of different types of electric devices working in closed systems indicate that they indeed produce small thrusts, consistent with the view that there are no truly closed systems if all systems are somehow connected by quantum-entanglement mechanisms. In such systems, the momentum conservation and Newton's third law are preserved.

The central point of this investigation is to show that the anomalous accelerations detected in the Pioneer spacecraft can be explained both qualitatively and quantitatively using a very simple calculation and a basic hypothesis consistent with our GQE theoretical framework. Within this framework, there is no closed system, since all particles in the Universe are quantum-entangled. In the Pioneer spacecraft, the anomalous effect can be described using only a few parameters of the onboard

TWTA, namely, the electron-beam current, the spacecraft mass, and the gain factor, yielding results in good agreement with the values experimentally observed.

Although thermal radiation asymmetry has also been proposed as an explanation for the anomaly, that explanation is based on several assumptions, estimates, simulations, and approximations. By contrast, the explanation proposed here is simpler and therefore consistent with Occam's razor, while still presenting good agreement with the acceleration observed experimentally. In fact, both the experimental and theoretical accelerations were of order 5×10^{-3} m/s², namely $a_{exp} = 0.00578$ m/s² and $a_{theor} = 0.00554$ m/s².

Author contributions

EP was responsible for the conception of the project, the laboratory experiments, calculations of the model, writing the initial draft of the work and check of the final version. VF was responsible for the analysis of the initial text and check of the calculations, as also writing the final version of the text, including the introduction and references.

Use of AI tools declaration

The authors declare they used the Artificial Intelligence (AI) tool Perplexity Pro in order to correct possible language errors or misprints in the creation of this article, after their own writing.

Conflict of Interest

The authors declare no conflict of interest.

References

1. Shawyer R (2015) Second Generation EmDrive Propulsion Applied to SSTO Launcher and Interstellar Probe. *Acta Astronautica* 116: 166–174. https://doi.org/10.1016/j.actaastro.2015.07.002
2. Fearn H, Woodward JF (2016) Breakthrough Propulsion I: The Quantum Vacuum. *J Brit Interplanetary Soc* 59: 155–162.
3. Brady DA, White HG, March P, et al. (2014) Anomalous Thrust Production from an RF Test Device Measured on a Low-Thrust Torsion Pendulum. *50th AIAA/ASME/SAE/ASEE Joint Propulsion Conference*, American Institute of Aeronautics and Astronautics. https://doi.org/10.2514/6.2014-4029
4. Buniy RV, Hsu SDH (2012) Everything is Entangled. *Phys Lett B* 718: 233–236. https://doi.org/10.1016/j.physletb.2012.09.047
5. Porcelli EB, Filho VS (2017) Anomalous effects from dipole-environment quantum entanglement. *Int J Adv Eng Res Sci* 4: 131–144. https://dx.doi.org/10.22161/ijaers.4.1.2
6. Wiesniak M, Vedral V, Brukner C (2005) Magnetic Susceptibility as a Macroscopic Entanglement Witness. *New J Phys* 7: 258. https://www.doi.org/10.1088/1367-2630/7/1/258
7. Porcelli EB, Filho VS (2016) On the Anomalous Forces in High-Voltage Symmetrical Capacitors. *Phys Essays* 29: 2–9. https://doi.org/10.4006/0836-1398-29.1.002

8. Porcelli EB, Filho VS (2020) Experimental Verification of Anomalous Forces on Shielded Symmetrical Capacitors. *Appl Phys Res* 12: 33–41. https://doi.org/10.5539/apr.v12n2p33
9. Porcelli EB, Filho VS (2019) Explaining Anomalous Forces in Microwave Cavities. *J Eng* 2019: 7279–7286. https://doi.org/10.1049/joe.2019.0011
10. Porcelli EB, Filho VS (2019) On the Possible Anomaly of Asymmetric Weight Reduction of Gyroscopes under Rotation. *Trends J Sci Res* 4: 29–38. https://doi.org/10.31586/MolecularPhysics.0401.05
11. Porcelli EB, Filho VS (2021) Characterization of anomalous forces in dielectric rotors. *Can J Phys* 99: 889–897. https://doi.org/10.1139/cjp-2020-0570
12. Porcelli EB, Filho VS (2017) Induction of Forces at Distance Performed by Semiconductor Laser Diodes. *Am J Eng Res* 6: 35–48. Available from: http://www.ajer.org/papers/v6(05)/F06053548.pdf.
13. Porcelli EB Induction of Force Performed by the Semiconductor Laser Diodes. US Patent No. US9,882,348B2, 2018.
14. Porcelli EB, Filho VS (2017) Theoretical study of anomalous forces externally induced by superconductors. *Nat Sci J* 9: 293–305. https://doi.org/10.4236/ns.2017.99028
15. Porcelli EB, Filho VS (2018) Analysis of Possible Nonlocal Forces in Superconducting Materials. *J Power Eng Eng* 6: 85–95. https://doi.org/jpee.2018.61007
16. Anderson JD, Laing PA, Lau EL, et al. (1998) Indication, from Pioneer 10/11, Galileo, and Ulysses Data, of an Apparent Anomalous, Weak, Long-Range Acceleration. *Phys Rev Lett* 81: 2858. https://doi.org/10.1103/PhysRevLett.81.2858
17. Rañada AF (2005) The Pioneer anomaly as acceleration of the clocks. *Found Phys* 34: 1955–1971. https://doi.org/10.1007/s10701-004-1629-y
18. Anderson JD, Laing PA, Lau EL, et al. (2002) Study of the anomalous acceleration of Pioneer 10 and 11. *Phys Rev D* 65: 082004. https://doi.org/10.1103/PhysRevD.65.082004
19. Katz JI (1999) Comment on "Indication, from Pioneer 10/11, Galileo, and Ulysses Data, of an Apparent Anomalous, Weak, Long-Range Acceleration". *Phys Rev Lett* 83: 1892. https://doi.org/10.1103/PhysRevLett.83.1892
20. Murphy EM (1999) A prosaic explanation for the anomalous accelerations seen in distant spacecraft. *Phys Rev Lett* 83: 1890. https://doi.org/10.1103/PhysRevLett.83.1890
21. Scheffer LK (2003) Conventional forces can explain the anomalous acceleration of Pioneer 10. *Phys Rev D* 67: 084021. https://doi.org/10.1103/PhysRevD.67.084021
22. Turyshev SG, Toth VT (2010) The Pioneer Anomaly. *Living Rev Relat* 13: 4. https://doi.org/10.12942/lrr-2010-4
23. Turyshev SG, Toth VT, Kinsella G, et al. (2012) Support for the Thermal Origin of the Pioneer Anomaly. *Phys Rev Lett* 108: 241101. https://doi.org/10.1103/PhysRevLett.108.241101
24. Toth VT, Turyshev SG (2009) Thermal Recoil Force, Telemetry and the Pioneer Anomaly. *Phys Rev D* 79: 043011. https://doi.org/10.1103/PhysRevD.79.043011
25. Braga NC, Valores médios e RMS para sinais (M177). Available from: https://www.newtoncbraga.com.br/matematica-na-eletronica/11083-valores-medios-e-rms-para-sinais-m177.html.
26. Aharanov Y, Bohm D (1959) Significance of Electromagnetic Potentials in the Quantum Theory. *Phys Rev* 115: 485. https://doi.org/10.1103/PhysRev.115.485

27. Becker M, Guzzinati G, Béché A, et al. (2019) Asymmetry and Non-Dispersivity in the Aharonov-Bohm Effect. *Nat Comm* 10: 1700. https://doi.org/10.1038/s41467-019-09609-9
28. Alsindi MS, Arbab IA (2022) On the Origin of a Longitudinal Force. *J Qassim University Science* 15: 68–77. https://jnsm.qu.edu.sa/index.php/jnm/article/download/2318/2353.
29. Adhikari KR (2014) Electrical Conductivity: Classical Electron and Quantum Mechanical Approaches. *Himalayan Phys* 5: 31–35. https://doi.org/10.3126/hj.v5i0.12833
30. Bueno MA, Assis AKT (2001) *Inductance and Force Calculations in Electrical Circuits*, Huntington, New York: Nova Science Publishers Inc.
31. Graneau N, Phipps Jr T, Roscoe D (2001) An experimental confirmation of longitudinal electrodynamic forces. *Eur Phys J* 15: 87–97. http://10.1007/s100530170186
32. Zeilinger A (1999) Experiment and the foundations of quantum physics. *Rev Mod Phys* 71: S288. https://doi.org/10.1103/RevModPhys.71.S288
33. Porcelli EB, Alves OR, Filho VS (2023) Detection of preexisting quantum entanglements between dipole-photon discrete observables. *Opt Quant Electron* 55: 944. https://doi.org/10.1007/s11082-023-05216-7
34. Lohmeyer WQ, Aniceto RJ, Cahoy KL (2016) Communication satellite power amplifiers: current and future SSPA and TWTA technologies. *Int J Satell Commun Network* 34: 95–113. https://doi.org/10.1002/sat.1098
35. Gilmour Jr AS (1994) *Principles of Traveling Wave Tubes,* Artech House Radar Library.
36. The Planetary Society (2025) Pioneer 10 or Pioneer 11. Available from: https://www.planetary.org/space-images/pioneer-10-or-pioneer-11.
37. Dornseif ER, Spica Jr A, Walters GC (1969) Development Program for 35 Watt Traveling - Wave Tube Space Amplifier. Report No. 69–4060R25, Watkins-Johnson Company. Available from: https://ntrs.nasa.gov/api/citations/19700017855/downloads/19700017855.pdf.
38. Hall CF, Smith MA (1971) Pioneer F/G: Spacecraft Operational Characteristics. Report. NASA/TP-2019-220324. Available from: https://ntrs.nasa.gov/api/citations/20190030279/downloads/20190030279.pdf.
39. Amos J (2018) Sonda New Horizons, da NASA: por que o 1º dia do ano promete ser histórico para a exploração espacial, Article BBC News. Available from: https://www.bbc.com/portuguese/geral-46720147.
40. Guerra AGC, Francisco F, Gil PJS, et al. (2017) Estimating the thermally induced acceleration of the New Horizons spacecraft. *Phys Rev D* 95: 124027. https://doi.org/10.1103/PhysRevD.95.124027
41. Minenna DFG, André F, Elskens Y, et al. (2019) The Traveling-Wave Tube in the History of Telecommunication. *Eur Phys J H EDP Sci* 44: 1–36. https://doi.org/10.1140/epjh/e2018-90023-1